Pharm Res (2015) 32:3415–3431
DOI 10.1007/s11095-015-1719-x

RESEARCH PAPER

Suppression of Remodeling Behaviors with Arachidonic Acid Modification for Enhanced *in vivo* Antiatherogenic Efficacies of Lovastatin-loaded Discoidal Recombinant High Density Lipoprotein

Hongliang He[1] • Mengyuan Zhang[1] • Lisha Liu[1] • Shuangshuang Zhang[1] • Jianping Liu[1] • Wenli Zhang[1]

Received: 9 March 2015 / Accepted: 19 May 2015 / Published online: 4 June 2015

ABSTRACT

Purpose A series of *in vitro* evaluation in our previous studies had proved that arachidonic acid (AA) modification could suppress the remodeling behaviors of lovastatin-loaded discoidal reconstituted high density lipoprotein (LT-d-rHDL) by restraining the reactivity with lecithin cholesterol acyltransferase (LCAT) for reducing undesired drug leakage. This study focuses on the investigation of AA-modified LT-d-rHDL (AA-LT-d-rHDL) in atherosclerotic New Zealand White (NZW) rabbit models to explore whether AA modification could enhance drug targeting delivery and improve antiatherogenic efficacies *in vivo*.

Methods After pharmacokinetics of AA-LT-d-rHDL modified with different AA amount were investigated in atherosclerotic NZW rabbits, atherosclerotic lesions targeting property was assessed by *ex vivo* imaging of aortic tree and drug distribution. Furthermore, their antiatherogenic efficacies were elaborately evaluated and compared by typical biochemical indices.

Results With AA modification amount augmenting, circulation time of AA-LT-d-rHDL was prolonged, and drug accumulation in the target locus was increased, eventually the significant appreciation in antiatherogenic efficacies were further supported by lower level of bad cholesterol, decreased atherosclerotic lesions areas and mean intima-media thickness (MIT), markedly attenuated matrix metalloproteinase-9 (MMP-9) protein expression and macrophage infiltration.

Conclusion This proof-of-concept study demonstrated that AA-LT-d-rHDL could enhance drug accumulation in atherosclerotic lesion and impede atherosclerosis progression more effectively.

KEY WORDS antiatherogenic efficacies · arachidonic acid modified d-rHDL · drug leakage · LCAT · remodeling behaviors

ABBREVIATIONS

AA	Arachidonic acid
AA-LT-d-rHDL	AA-modified rHDL loaded with lovastatin
apoA-I	Apolipoproteina-I
DL	Drug loading efficiency
d-rHDL	Discoidal recombinant HDL
EE	Entrapment efficiency
HDL	High density lipoprotein
HDL-C	High density lipoprotein cholesterol
LCAT	Lecithin cholesterol acyltransferase
LDL-C	Low density lipoprotein cholesterol
LT-d-rHDL	Lovastatin-loaded rHD
MIT	Intima-media thickness
MMP-9	Matrix metalloproteinase-9
RCT	Reverse cholesterol transport
rHDL	Recombinant HDL
s-rHDL	Spherical recombinant HDL
TC	Total cholesterol
TG	Triglyceride

INTRODUCTION

Atherosclerosis is a major cause of disability and mortality worldwide. It has been generally acknowledged that rupture of vulnerable plaques and ensuing thrombosis constitute the most important contributors to acute coronary syndrome in the advanced atherosclerosis, such as acute myocardial infarction and stroke (1). Statins, the most widely used anti-atherosclerotic agents, was considered to reduce cardiovascular risks mainly due to their

Hongliang He and Mengyuan Zhang contributed equally to this work.

✉ Jianping Liu
jianpingliu1293@163.com

✉ Wenli Zhang
jianpingliu1293@163.com

[1] Department of Pharmaceutics, China Pharmaceutical University
No.24, Tongjia Lane, Nanjing 210009, People's Republic of China

excellent lipid-lowering effect in the past years. Recently, a growing number of studies have highlighted the nonlipid-lowering benefits of statins, including antioxidant effect, improving or restoring the endothelial function, inhibiting platelet aggregation, anti-thrombotic property and favoring the stability of vulnerable plaques, *etc.* (2). However, the nonlipid-lowering effects of statins are greatly hindered by their poor systemic bioavailability and adverse effects after being administrated orally for a long time (3). Therefore, exploitation of novel drug delivery system to efficiently deliver statins into the atherosclerotic plaques, thus better inhibiting the progression of plaques and stabilizing the vulnerable plaques as well as reducing potential side effects, will be a promising approach for treatment of atherosclerosis in future.

High density lipoprotein (HDL) is functional plasma lipoprotein with two structural forms, the discoidal and the spherical. Nascent discoidal HDL (d-HDL) could efficiently remove cholesterol from cells of peripheral tissues and covert into mature d-HDL, subsequently transformed into spherical HDL (s-HDL) under the catalysis of lecithin cholesteryl acyltransferase (LCAT), and those above whole processes are referred as remodeling behaviors. Ultimately, the lipid core of s-HDL is selectively endocytosed by liver mediated by the scavenger receptor class B type I (SR-BI) which is known as HDL receptor (4). This process of transferring peripheral cholesterol into liver for excretion is termed as reverse cholesterol transport (RCT), which has been generally demonstrated as an important mechanism in prevention of cardiovascular disease such as atherosclerosis. Additionally, there are some other acknowledged biological activities for HDL such as anti-inflammation (5), anti-oxidation (6) as well as enhancement of the nitric oxide (NO) production (4), *etc.*

Reconstituted HDL (rHDL), composed of commercially available lipids and serum-derived or recombinant apolipoprotein, has been increasingly developed as ideal drug delivery system for anti-tumor agents (7), RNA (8, 9) and cardiovascular drugs (10, 11) due to its attractive functions of endogeneity, biodegradability and selectively SR-BI receptor-mediated endocytosis (12). Among our previous studies (10, 11, 13–15), two kinds of rHDL, d-rHDL and s-rHDL, loading with various kinds of cardiovascular drugs, had been constructed. It was proved that both d-rHDL and s-rHDL could greatly improve the pharmacokinetic behaviors and bioavailability of free drug. Especially, the antiatherogenic efficacy would be markedly enhanced in combination with the biofunctional properties of rHDL as cardiovascular drug carriers. However, our previous studies (13, 16) found that once encountered with LCAT both *in vitro* and *in vivo*, drug-loaded d-rHDL would experience the similar remodeling process as the native d-HDL. And during this structural conversion from the discoidal to the spherical, a large amount of drugs encapsulated in d-rHDL could leak out, which decreased the drug delivery to the target site and lowered the efficacy.

Recently, we have explored some effective approaches to decrease the undesired drug leakage of d-rHDL during the remodeling behaviors, such as modified-cholesterol and modified apoA-I (17–19). However, those approaches needed some elaborate and complicated chemical processes, which aroused us to develop more simple and feasible way to achieve the goal. Lately in our report, we had demonstrated that *via* simple self-assembly, arachidonic acid (AA)-modified d-rHDL loaded with lovastatin, defined as AA-LT-d-rHDL, had lower reactivity with LCAT, which was proved by a series of evaluations of *in vitro* remodeling behaviors induced by LCAT, more efficient intracellular drug delivery and more potent inhibitory effect on the formation of macrophage-derived foam cell than unmodified LT loaded d-rHDL (LT-d-rHDL) (19). The roles of AA modification in remodeling suppression lies in two aspects: 1) the increased negative charge of d-rHDL after AA insertion repelled the attachment of LCAT, and then lowered the reactivity of AA-LT-d-rHDL with LCAT (20); 2) AA insertion could increase the fluidity of phospholipids bilayer of d-rHDL which would weaken the insertion degree of apoA-I in phospholipids bilayer of d-rHDL, alter spatial structure of uninserted apoA-I in d-rHDL and shield the activation sites for LCAT on the apoA-I (21, 22).

Based on our previous findings, in the current study, the antiatherogenic efficacies of AA-LT-d-rHDL in the atherosclerotic New Zealand White (NZW) rabbits were further studied (The whole contents were summarized graphically in Fig. 1). Specifically, four AA-LT-d-rHDL modified without or with different AA amount were constructed and characterized: LT-d-rHDLs without AA insertion, 1:20 AA-LT-d-rHDL (AA:phospholipids mole ratio, 1:20), 1:10 AA-LT-d-rHDL (AA:phospholipids mole ratio, 1:10) and 1:5 AA-LT-d-rHDL (AA:phospholipids mole ratio, 1:5). Moreover, atherosclerotic lesions targeting property was investigated by *ex vivo* imaging of aortic tree and drug distribution in atherosclerotic lesions respectively. Furthermore, their antiatherogenic efficacies were elaborately evaluated and compared by typical biochemical indices including serum lipid levels, atherosclerotic lesions size areas, mean intima-media thickness (MIT), and degrees of matrix metalloproteinase-9 (MMP-9) expression and macrophage infiltration in the aortic tree being susceptibly induced to form atherosclerosis, respectively. This study may provide some valuable references to better utilize d-rHDL as drug delivery system..

MATERIALS AND METHODS

Materials

Lovastatin was kindly donated by Jiangsu Yangzi River Pharmacy Company (China). AA, Cholesterol, cholesteryl oleate and oil red O were purchased from Sigma-Aldrich

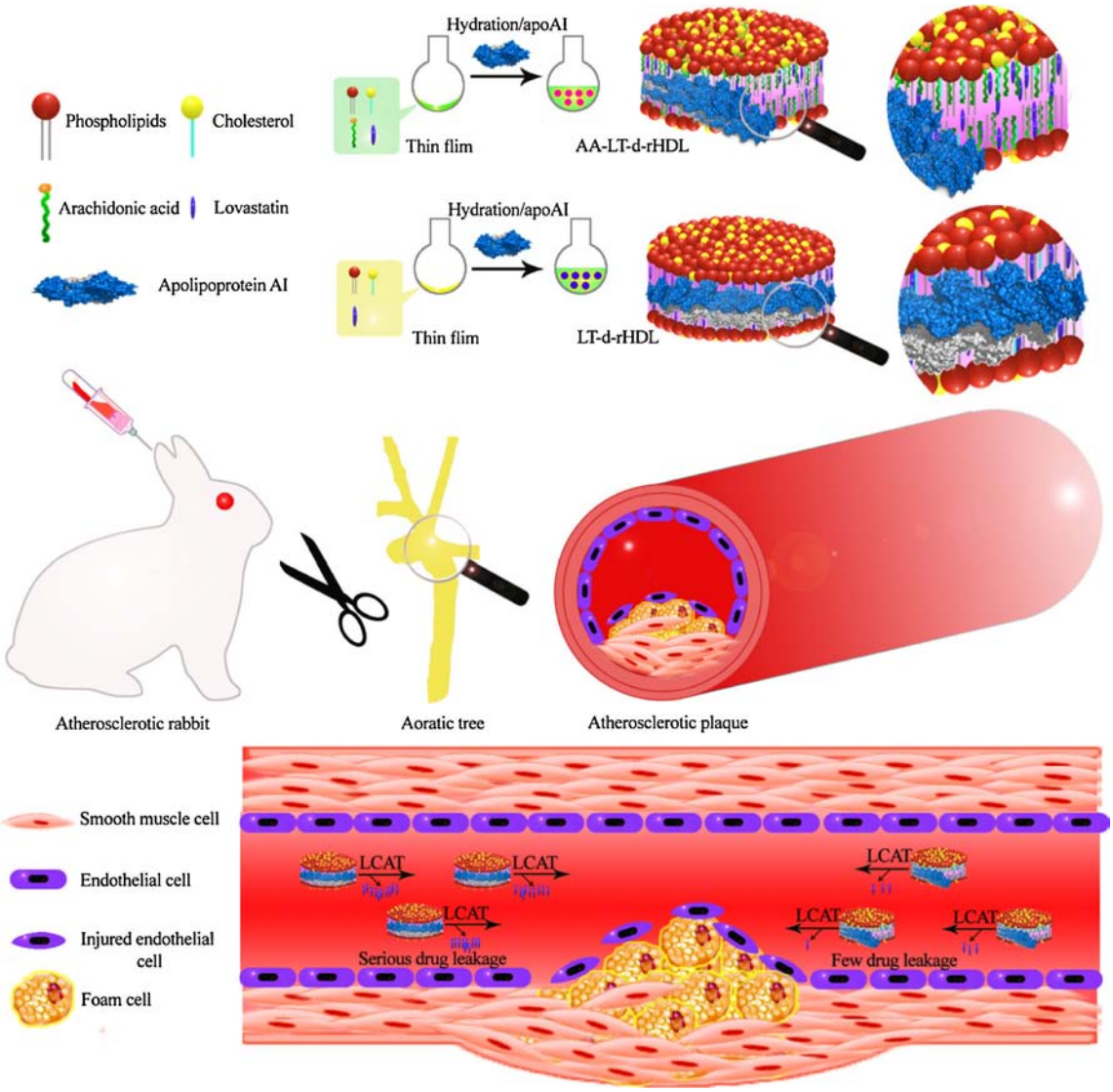

Fig. 1 Schematic diagram on preparation methods and atherosclerotic lesion delivering property of AA-LT-rHDL

(USA). Lipoid S 100 was obtained from Lipoid GmbH (Germany). The whole apolipoproteins (apos, 97% pure of apoA-I) were isolated from the industrial waste during production of albumin by our laboratory (as described previously). Bovine serum albumin (BSA) was purchased from Sun Shine Biotech Co. Ltd. (China). DiR was purchased from FanboBiochemicals Co. Ltd. (China).LT Capsule (LT-Capsule, purchased from ChengduYongkang Pharmacy Co., Ltd., China). HPLC-grade reagents were used as the mobile phase in HPLC analysis, and all other reagents were of analytical grade. Distilled and deionized water were used in all experiments.

Preparation of Different AA-LT-d-rHDL

LT-d-rHDL and three AA-LT-d-rHDL were prepared as liposome formation followed by sodium cholate-mediated method (13, 19). Briefly, LT-Liposome and AA-modified LT-Liposome were prepared firstly and used as the lipid cores. LT-d-rHDL and AA-LT-d-rHDL were obtained by incubating the lipid cores with apos accordingly.

LT-Liposome and AA-LT-Liposome were prepared by thin-film dispersion method. Briefly, LT, different AA modification amount (AA/phospholipids mole ratio, 0/1:20/1:10/1:5), Lipoid S-100 and cholesterol were dissolved in appropriate volume solution consisting of methanol/chloroform (1:1, V/V) and dried in an eggplant-shaped flask under vacuum at 30±2°C. 15 mL of 0.02 M Tris–HCl buffer (pH 8.0) was added into the flask to hydrate the dry film, then the mixture was vortexed thoroughly for 10 min at 30±2°C, followed by ultrasonication for 200 s at 300 W on ice using an Ultrahomogenizer JY92II (Ningbo, China) till occurrence of a clear suspension. The dispersions were then filtrated through 0.22 μm filter to remove larger particles.

LT-Liposome and AA-LT-Liposome obtained above were incubated with equivalent volume pH 8.0 Tris–HCl buffer containing 24 mg apos and 48 mg sodium cholate under 600 rpm at 4°C for 12 h to form LT-d-rHDL and AA-LT-d-rHDL, respectively. After incubation, the dispersions were dialyzed against pH 8.0 Tris–HCl for 48 h to remove excess sodium cholate and unloaded drug.

Additionally, as the control in the following antiatherogenic efficacy evaluation in atherosclerotic rabbits, reconstituted s-HDL (s-rHDL) loaded with LT (LT-s-rHDL) was also prepared as described previously in those studies (10, 13, 14).

In vitro Characterizations

Mean sizes and zeta potentials of the LT-d-rHDL and three AA-LT-d-rHDL preparations were measured by dynamic light scattering (DLS) analyzer (Zetasizer 3000 HAS, Malvern, UK) in triplicate. All Samples were diluted appropriately with aqueous phase before measurement.

The entrapment efficiency (EE%) and drug-loading coefficient (DL%) were quantified and calculated as microcolumn separation method (17–19) and the following equations,

$$EE(\%) = \frac{W}{W_t} \times 100\% \quad (1)$$

$$\mathrm{DL}\ (\%)\ = \frac{Q}{Q_t} \times 100\% \quad (2)$$

Where W and Wt are the amount of drug in each preparation after and before passing through the microcolumn, respectively; where Q means the drug content in each preparation and Qt means the total amount of the feeding materials.

Transmission electron microscopy (TEM, H-7650, Hitachi High-Technologies Corporation, Japan) was employed to characterize visually LT-d-rHDL and three AA-LT-d-rHDL preparations (19).

Establishment of Atherosclerotic Animal Models

Male NZW rabbits weighing 2.0–2.2 kg were obtained from Qinglong Mountain Animal center (Nanjing, China). Atherosclerotic NZW rabbits were induced by us *via* in combination endothelial injury and high-fat diets (13). Specifically, NZW rabbits were individually housed in a controlled environment maintained at 19°C with food and water provided *ad libitum*. After being fed with normal diet for 2 weeks, NZW rabbits were injected intravenously with 100 mg/kg BSA every other day for three times in order to induce endothelial injury, then fed with high-fat diet (2% cholesterol, 10% dried egg yolk, 5% lard, 0.3% sodium cholate and 0.2% propylthiouracil) for 16 weeks to develop atherosclerotic NZW rabbits. All care and handling of animals were approved by the Institutional Animal Care and Use Committee at China Pharmaceutical University and carried out in strict accordance with the National Institute of Health Guide for the Care and Use of Laboratory Animals.

Ultimately, intima-media thickness (IMT) of carotid artery detected by Color Doppler ultrasound imaging (PHILIPS, Netherlands), photographs of aortic tree and representative histological sections of the aortic arch stained by H&E all indicated the typical pathological features of atherosclerotic lesions (data were not presented here), which testified the successful establishment of atherosclerotic NZW rabbit models.

Pharmacokinetics in Atherosclerotic Rabbits

Forty-eight atherosclerotic NZW rabbits were randomly divided into the following eight groups (6 rabbits per group), respectively: (1) commercially available LT-Capsule (as a commercial reference preparation); (2) LT-Solution (dissolved in 50% dimethyl sulfoxide in normal saline); (3) LT-Liposome; (4) LT-d-rHDL; (5) 1:20AA-LT-d-rHDL; (6) 1:10AA-LT-d-rHDL; (7) 1:5AA-LT-d-rHDL and (8) LT-s-rHDL. The LT concentration of above eight different LT preparations was around 1.1 ~ 1.3 mg/mL. LT-Capsules (LT dose of 20 mg/kg) were orally administrated and the other seven LT preparations (LT dose of 2 mg/kg) were administrated through the marginal ear vein intravenously. Then the blood samples (1.5 mL) were collected from the marginal ear vein at 15 min, 30 min, 1 h, 2 h, 4 h, 8 h, 12 h, 24 hand 36 h after the administration, respectively. The plasma was obtained by centrifugation at 3000 rpm for 10 min and stored at −20°C prior to analysis.

Plasma concentrations of LT were determined by validated reverse-phase high performance liquid chromatography (HPLC) with UV detection. Briefly, 0.4 mL plasma samples were extracted with 3 mL of acetic ether. After 3 min vortex, the total organic layer was separated by centrifugation at 3000 rpm for 10 min and transferred to a 10 mL tube and dried under nitrogen at 40°C. Then the residues were reconstituted by 100 μL methanol and vortexed for 2 min. After centrifugation at 12,000 rpm for 10 min, 20 μL of supernatant were subjected into HPLC analysis using Agilent 1260 series (Palo Alto, CA, USA) with a Hypersil ODS column (4.6 × 250 mm, 5 μm) kept at 30°C. The analysis was carried out with a (65:35; v/v) mobile phase of acetonitrile:10 m Ammonium acetate (pH 4.0). The flow rate was kept at 1 mL/min and the effluent was monitored at 238 nm (23).

Atherosclerotic Lesions Targeting Properties

Ex vivo Imaging Studies

Liposome, d-rHDL, three AA-d-rHDL preparations and s-rHDL loaded with near-infrared fluorescent dye DiR only instead of LT were prepared as described above section "Preparation of Different AA-LT-d-rHDL", respectively, and then were employed in the following *ex vivo* imaging of aortic tree.

Eighteen atherosclerotic rabbits ($n=3$) and 18 normal rabbits ($n=3$) were administrated i.v. *via* marginal ear vein of DiR formulations at a dose of 0.3 mg/kg:DiR-L, DiR-d-rHDL, 1:20AA-DiR-d-rHDL, 1:10AA-DiR-d-rHDL, 1:5AA-DiR-d-rHDL and DiR-s-rHDL. After 4 h, all rabbits were euthanized and dissected. Then the intact aortic trees were taken out, stripped off fats and tissues adhering to the adventitia, and rinsed with saline until no blood. Each gained aortic tree was visualized using Kodak *in vivo* imaging system FX PRO (Kodak, USA) equipped with an excitation bandpass filter at 730 nm and an emission at 790 nm. Laser power and count time settings were optimized at 40 μW and 0.3 s per point. Images were analyzed using the Kodak Molecular Imaging Software 5.X (13, 24, 25).

Tissue Distribution in the Atherosclerotic Rabbits

Group regimens were set up uniformly as the above mentioned in the section "Pharmacokinetics in Atherosclerotic Rabbits" and subjected to the following treatment. Specifically, LT-Capsule was administrated orally at dose of 20 mg/kg and the other seven preparations were intravenously administrated *via* marginal ear vein at a dose of 2 mg/kg. After 0.5 h and 4 h injection, rabbits were euthanized *via* an overdose of intravenous pentobarbital (three rabbits for each time point in each group). The blood, heart, liver, spleen, lung, kidney and atherosclerotic lesion were collected, respectively. All tissue samples were thoroughly rinsed with ice-cold saline, dried with filter paper to remove excess fluid, weighed, cut into small pieces, homogenized using XHF-D high speed disperser form Ningbo Scientz Biotechnology Co. Ltd. (China) in 100 mM potassium phosphate (pH 7.4) to dilute into 250 mg tissue/mL homogenates and stored at −20°C prior to determination. 1 mL of each tissue homogenate and 0.4 mL of plasma were extracted with 4 mL and 3 mL of acetic ether, respectively, and were subjected to the following disposal same as described previously in the above section "Pharmacokinetics in Atherosclerotic Rabbits" (23, 26). The methodology for LT analysis in blood and tissues has been validated, which were line with the requirements of *in vivo* determination.

Antiatherogenic Efficacy in Atherosclerotic Rabbits

Briefly, 48 NZW rabbits were randomly divided into the eight groups ($n=6$) same with the above mentioned in the section "Pharmacokinetics in Atherosclerotic Rabbits", and dose of 8 mg/kg was orally administrated and the other seven LT preparations were intravenously administrated through the marginal ear vein at a dose of 0.4 mg/kg for the further 8 weeks after being fed with 8 weeks high-fat diet without any drug intervention. While the animals induced to form atherosclerosis and without any treatments were taken as the positive control group, the normal NZW rabbits were taken as the negative control group, and the atherosclerotic rabbits with administration were taken as treatment groups. Then all groups were subject to the following tests so as to evaluate and compare antiatherogenic efficacies of different LT preparations (27–29).

Blood Lipid Levels

Blood of rabbits (2 mL) from all groups was obtained *via* marginal ear vein after 8 weeks administration. Serum levels of total cholesterol (TC), triglyceride (TG), high density lipoprotein cholesterol (HDL-C), and low density lipoprotein cholesterol (LDL-C) were measured by CHOD-PAP method, respectively (Roche Diagnostics, Mannheim, Germany) (30).

Atherosclerotic Lesions Areas

Briefly, the each entire aorta above the iliac artery from all groups was removed, and all fats and tissues adhering to the adventitia were peeled off from the aorta. Then two centimeters thoracic aorta from the same position from each sample was scissored correspondingly, opened along their ventral surface and stained with oil red O in 60% propylene glycol for 3 ~ 4 h at room temperature, then were differentiated in 60% propylene glycol for 6 ~ 7 times until the atherosclerotic lesions were stained red and the vessel wall white, then observed by EOS 5D Mark III (Canon, Japan) (13, 31).

The lesions positive staining (%), defined as the atherosclerotic lesions areas in the whole aorta zone, was used as an index to evaluate the extent of lesions in the aortas of atherosclerotic rabbits, which was quantified by Image-pro plus 6 (IPP 6).

Mean Intima-Media Thickness

The corresponding segment (aortic arch) from each sample was dissected, fixed overnight in 10% buffered formalin, imbedded in paraffin, sliced as 5-μm-thick tissue section and stained with hematoxylin and eosin. The histological sections were evaluated by an experienced pathologist blinded to treatment. Quantitative evaluation was performed with the use of an Olympus BH-2 microscope equipped with an eyepiece micrometer. The degree of intimal atheromatous involvement

was determined by mean intima-media thickness (MIT, μm) (32, 33).

Immunostaining for MMP-9 and Macrophage Expression in the Atherosclerotic Lesions

Immunofluorescence for MMP-9 was carried out according to the previous reports with minor modification. Shortly, freshly frozen aortic arches were sectioned into 5 μm-thick pieces, which were blocked in 5% normal goat serum (Sigma) and 0.01% Triton X-100 in PBS, and then incubated with primary antibody mouse monoclonal to MMP-9 (Abcam) overnight at 4°C. Sections were rinsed in PBS buffer for 4 times and incubated with secondary antibody for 1 h. The Sections were rinsed with PBS buffer for 4 times and counterstained with mounting media containing DAPI. Sections were examined by using an Olympus DP70 fluorescence microscope (Olympus, Tokyo, Japan). Images from 5 to 8 randomly selected visual fields (magnification, 200×) per aortic section were captured, and the positive signal (positive cells or positive-staining area, without selecting autofluorescent elastic fibers) and the evaluated area were measured by using IPP 6. The positive signals were normalized to the evaluated aortic area, and the mean positive signals were calculated and compared between groups (34, 35).

Immunohistochemistry for macrophage were carried out as reported previously with minor revisions. Briefly, paraffin-embedded aortic arches were cross-sectioned correspondingly from each sample into 4 μm thick pieces, dewaxed, and rehydrated. Endogenous peroxidase activity in the sections was quenched by incubation in 3% hydrogen peroxide: methanol (1:1) for 30 min. Nonspecific antibody binding was blocked by incubating the tissue section for 1 h in suppressor serum consisting of 6% goat serum and 4% BSA in PBS (pH 7). RAM-11 as the primary antibody for macrophage (1:50 in 1% goat serum and 4% BSA in PBS) was applied overnight at 4°C. Secondary antibodies diluted 1:100 in 4% BSA were applied for 30 min, then sections were stained with 3,3'-diaminobenzidine tetrahydrochloride (DAB, DAKO) at room temperature. Finally, sections were counterstained with hematoxylin and observed. Quantification was assessed by IPP 6 and expressed as positive staining (%) for macrophage infiltration (36, 37).

Western Blotting Analysis for MMP-9 and Macrophage Expression

Briefly, 1 cm aortic arches harvested correspondingly from each group were snap frozen in liquid nitrogen and subsequently homogenized in lysis buffer (50 mM Tris–HCl, pH 8.0, 150 mM NaCl, 0.02% sodium azide, 0.1% SDS, PMSF 100 mg/ml, aprotinin 1 mg/mL 1% NP-40, 0.5% sodium deoxycholate) with freshly added protease inhibitor using a tissue homogenizer. The homogenate was centrifuged and analyzed for protein content using a Bradford assay (Bio-Rad, CA). Equal amount of whole proteins were separated on an 8% SDS-polyacrylamide gel electrophoresis and transferred to polyvinylidene difluoride filters using an electroblotting apparatus. Filters were treated in Tris-buffered saline (pH 7.2) containing 0.1% Tween20 and 5% Bovine Serum Albumin for 1 h and incubated with specific monoclonal antibody against rabbit macrophages RAM-11 (DAKO) or mouse monoclonal against MMP-9 (Abcam) overnight at 4°C. The membrane was subsequently probed with a corresponding secondary antibody and visualized using the enhanced chemiluminescence system (Amersham; Buckinghamshire, United Kingdom). Furthermore, densitometry was analyzed and expressed as N-fold v.s. GAPDH (Abcam) (34, 38).

Statistical Data Analysis

Drug and Statistics for Windows (DAS 2.0) was utilized to analyze the pharmacokinetic data for each formulation. Comparisons of parameters between two groups were performed with unpaired Student *t* test, while comparisons of parameters among multiple groups were made with a one-way ANOVA analysis with $p<0.05$ set as statistically significance. All results were expressed as mean ± standard error unless otherwise indicated.

RESULTS

In vitro Characterizations

The mean sizes, zeta potentials, EE % and DL % of four LT-d-rHDL preparations with different AA modification amount, analyzed by DLS analyzer and HPLC assay, were depicted specifically in the following Table I, respectively. It could be inferred that as AA modification amount increased, both mean size and negative zeta potential of nanocarriers were markedly increased correspondingly. While the EE % and DL % were not significantly changed with the increment of AA amount. All those results were consistent with our previous reports (13, 19).

Visualized by TEM in the Fig. 2, all of four LT-d-rHDL preparations with different AA modification amount had the typical multi-discoidal structure similar to the native counterpart d-HDL, which was also consistent with our previous studies (13, 16, 17, 19). Meanwhile, there was no significant micro-structural difference among those four kinds of LT-d-rHDL preparations, and the sizes were basically consistent with those results obtained by DLS analyzer.

Table I Mean Sizes, Zeta Potential, EE % and DL % of four Different LT-d-rHDL Preparations (mean value ± SD, $n = 3$).

	LT-d-rHDLs	1:20 AA-LT-d-rHDLs	1:10 AA-LT-d-rHDLs	1:5 AA-LT-d-rHDLs
Mean size (nm)	44.5 ± 2.2	53.4 ± 1.7$^{\bullet}$	56.4 ± 0.9	59.2 ± 1.5§
Zeta potential (mV)	−12.89 ± 0.92	−18.42 ± 1.76$^{\bullet}$	−25.06 ± 1.44$^{\blacklozenge}$	−30.59 ± 1.87§
EE (%)	90.9 ± 0.8	90.5 ± 0.7	91.2 ± 0.4	90.6 ± 0.3
DL (%)	4.1 ± 0.4	4.0 ± 0.3	4.1 ± 0.2	3.9 ± 0.2

Significant differences: $\bullet p < 0.05$, compared 1:20 AA-LT-d-rHDL with LT-d-rHDL; $\blacklozenge p < 0.05$, compared 1:10 AA-LT-d-rHDL with 1:20 LT-d-rHDL; $\S p < 0.05$, compared 1:5 AA-LT-d-rHDL with 1:10 LT-d-rHDL

Pharmacokinetics in Atherosclerotic Rabbits

The plasma concentration-time profiles and related pharmacokinetic parameters of LT preparations in atherosclerotic rabbits are shown in Fig. 3 and in Table II, respectively. As shown in Fig. 3, almost no LT was found for both LT-Capsule and LT-Solution after 24 h administration, while LT was still detectable even after 36 h administration of LT-Liposome, LT-d-rHDL, 1:20 AA-LT-d-rHDL, 1:10 AA-LT-d-rHDL, 1:5 AA-LT-d-rHDL and LT-s-rHDL. Seen from Table II, the values of the area under the plasma concentration curve ($AUC_{0-\infty}$) for LT-Capsule were only 5.964 ± 1.992 mg/L/h compared with 12.206 ± 3.245 mg/L/h for LT-Solution, while the $AUC_{0-\infty}$ for LT-Liposome, LT-d-rHDL, 1:20 AA-LT-d-rHDL, 1:10 AA-LT-d-rHDL, 1:5 AA-LT-d-rHDL and LT-s-rHDL were increased by 3.53, 5.65, 5.89, 6.75, 7.37 and 7.09-fold, respectively. The corresponding mean residence time (MRT) increased 2.85, 4.41, 4.61, 4.80, 5.06 and 4.89-fold compared to that of LT-Solution, respectively, whereas the corresponding total body clearance (CL) were 3.64, 5.66, 6.07, 6.83, 7.45 and 6.83-fold lower than that of LT-Solution, respectively.

Atherosclerotic Lesions Targeting Properties

Ex vivo Imaging Studies

4 h after intravenous administration, it was obvious that the fluorescence signals intensity of aortic tree in the atherosclerotic rabbits were all much stronger than that in normal rabbits (Fig. 4). There was no significant difference among the fluorescence signals in the normal rabbits among all treatment groups. In the atherosclerotic rabbits groups, DiR-d-rHDL had stronger fluorescence signals than DiR-Liposome,

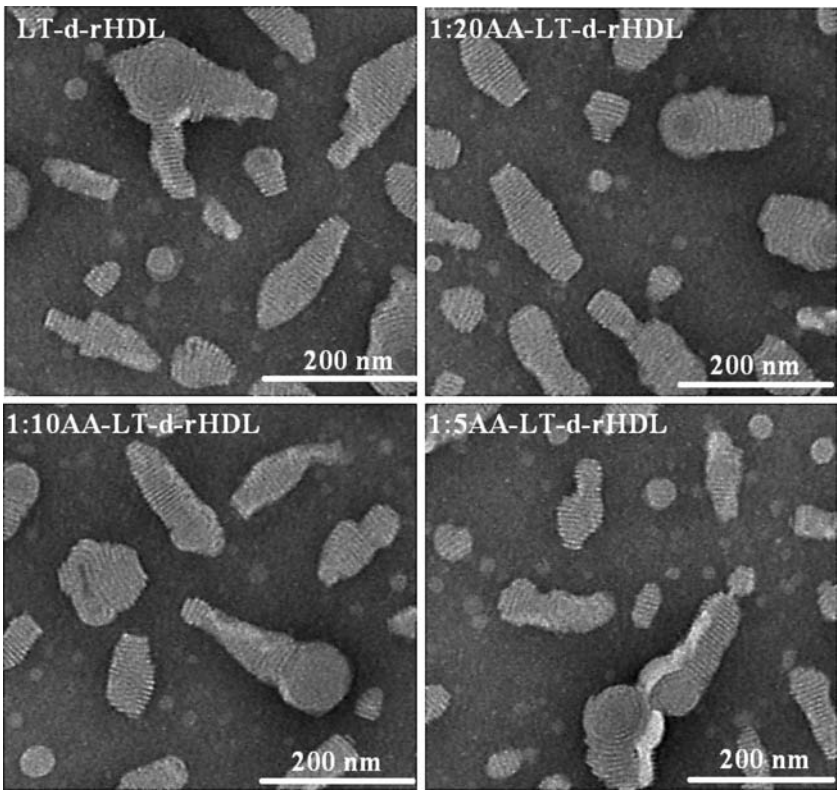

Fig. 2 TEM photographs of LT-d-rHDL, 1:20 AA-LT-d-rHDL, 1:10 AA-LT-d-rHDL and 1:5 AA-LT-d-rHDL

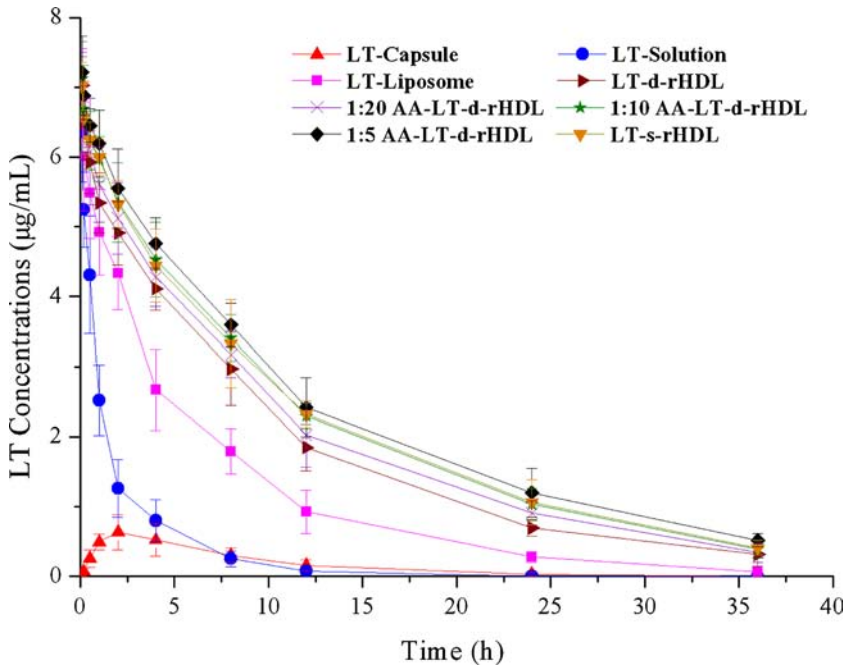

Fig. 3 Plasma concentration-time curves of LT after administration of LT-Capsule, LT-Liposome, LT-d-rHDL, 1:20AA-LT-d-rHDL, 1:10AA-LT-d-rHDL, 1:5AA-LT-d-rHDL and LT-s-rHDL in atherosclerotic NZW rabbits (mean value ± SD, $n = 6$)

however lower than that of DiR-s-rHDL. Furthermore, with the AA modification amount increased, the fluorescence signals in the atherosclerotic rabbits were gradually enhanced. It was worth noting that the fluorescence signals of aortic tree in the atherosclerotic rabbit treated with 1:5AA-DiR-d-rHDL were higher than that treated with DiR-s-rHDL.

Tissue Distribution in the Atherosclerotic Rabbits

As shown in the Fig. 5, after 0.5 and 4 h oral administration of LT-Capsule, the LT concentration were the lowest in each tissue. For LT-Solution, due to without any selectivity, there were no significant difference among the LT concentrations of various tissues, while LT-Liposome had higher LT concentration in both liver spleen due to the uptake by reticular endothelial system (RES). The plasma LT concentration at 4 h in the group treated with LT-Solution was significantly decreased compared with that at 0.5 h. Both after 0.5 and 4 h administration, the LT concentrations in atherosclerotic lesions from low to high in order was LT-Capsule, LT-Solution LT-Liposome, LT-d-rHDL, 1:20 AA-LT-d-rHDL, 1:10 AA-LT-d-rHDL or LT-s-rHDL, and 1:5 AA-LT-d-rHDL, respectively. Moreover, 4 h post-injection in the groups treated with nanostructured drug delivery systems, LT concentrations were on the decline in tissues except plaques, indicating enhanced atherosclerotic lesions-targeted

Table II Pharmacokinetic Parameters of LT in Different Formulations after *iv.* Administration (mean value ± SD, $n = 6$)

Formulations	$t_{1/2\ \alpha}$	$t_{1/2\beta}$	V_d (L/kg)	$AUC_{0-\infty}$ (mg/L/h)	$MRT_{0-\infty}$ (h)	CL (L/h/kg)
LT-Capsule	1.269 ± 0.566	5.291 ± 2.052	17.072 ± 6.322	5.964 ± 1.992	7.753 ± 1.083	3.354 ± 0.876
LT-Solution	0.528 ± 0.281	3.349 ± 1.376	0.298 ± 0.087	12.206 ± 3.245$^{\#}$	2.621 ± 1.763	0.164 ± 0.063
LT-Liposome	0.046 ± 0.013	4.417 ± 1.231	0.207 ± 0.116	42.048 ± 5.283$^{\triangledown}$	7.493 ± 2.212	0.045 ± 0.015
LT-d-rHDL	0.167 ± 0.074	7.669 ± 1.272	0.268 ± 0.125	68.952 ± 12.326§	11.524 ± 0.881§	0.029 ± 0.013
1:20AALT-d-rHDL	0.138 ± 0.024	8.098 ± 1.118	0.265 ± 0.075	71.625 ± 14.238	12.047 ± 1.242	0.027 ± 0.007
1:10AALT-d-rHDL	0.101 ± 0.013	8.544 ± 0.654	0.259 ± 0.131	82.446 ± 15.625	12.577 ± 0.715	0.024 ± 0.006
1:5AALT-d-rHDL	0.289 ± 0.123	9.204 ± 1.234	0.273 ± 0.074	89.826 ± 11.342※	13.271 ± 0.686※	0.022 ± 0.012
LT-s-rHDL	0.595 ± 0.262	9.047 ± 0.448	0.287 ± 0.106	86.548 ± 10.252$^{\blacktriangledown}$	12.837 ± 0.761$^{\blacktriangledown}$	0.024 ± 0.005

$t_{1/2\ \alpha}$, distribution half life; $t_{1/2\beta}$, elimination of half life; V_d, apparent volume of distribution; $AUC_{0-\infty}$, the area under the plasma concentration curve; $MRT_{0-\infty}$, mean residence time; CL, total body clearance

Significant differences: #$p < 0.05$, compared LT-Capsule with LT-Solution, ▽$p < 0.05$, compared LT-Liposome with LT-Solution, §$p < 0.05$, compared LT-d-rHDL with LT-Liposome, ※$p < 0.05$, compared 1:5AALT-d-rHDL with LT-d-rHDL, ▼$p < 0.05$, compared LT-d-rHDL with LT-s-rHDL

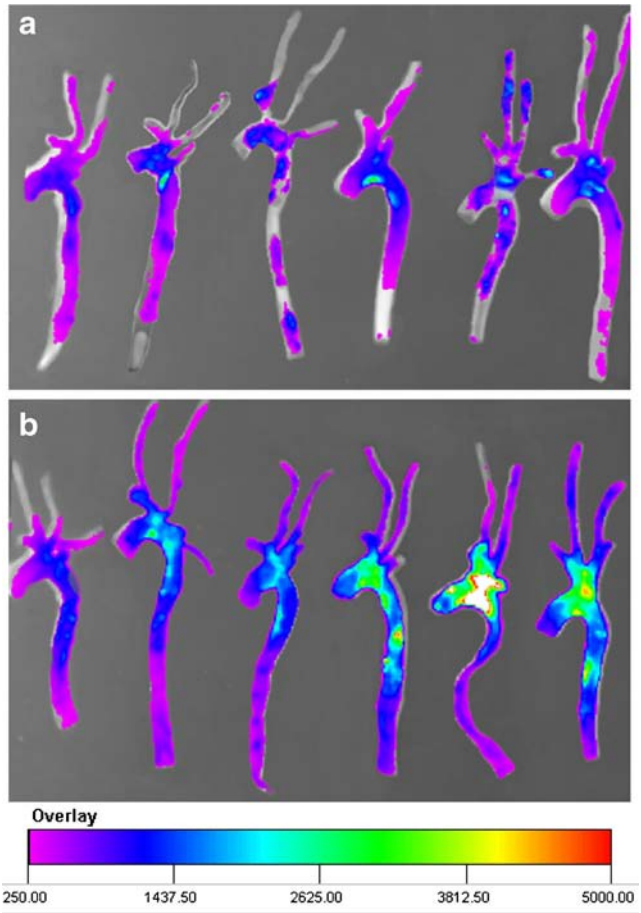

Fig. 4 *Ex vivo* imaging of the aortic trees from atherosclerotic (**a**) and normal (**b**) NZW rabbits administrated with DiR-Liposome, DiR-d-rHDL, 1:20AA-DiR-d-rHDL, 1:10AA-DiR-d-rHDL, 1:5AA-DiR-d-rHDL and DiR-s-rHDL, respectively (from the left to the right)

property *via* the extended circulation time by nanocarriers drug systems, especially for 1:5 AA-LT-d-rHDL.

Antiatherogenic Efficacy in Atherosclerotic Rabbits

Blood Lipid Levels

The blood lipid levels of different intervened-groups are provided in Table III. Compared with negative control group, levels of TC, TG and LDL-C (considered as bad cholesterol) were significantly higher in positive control group. And in treatment groups, levels of TG and LDL-C were gradually declined in the order of LT-Capsule, LT-Liposome, LT-d-rHDL and LT-s-rHDL. Furthermore, with the increment of AA modification amount, TC and LDL-C in LT-d-rHDL, 1:20 AA-LT-d-rHDL, 1:10 AA-LT-d-rHDL and 1:5 AA-LT-d-rHDL had been gradually lowered. In contrast, compared with other intervened-groups, levels of the HDL-C (known as good cholesterol) were evidently elevated in LT-d-rHDL, 1:20 AA-LT-d-rHDL, 1:10 AA-LT-d-rHDL, 1:5 AA-LT-d-rHDL and LT-s-rHDL groups.

Atherosclerotic Lesions Areas

Atherosclerotic lesions stained with oil red O in aortic arch and lesions positive staining (%) were presented in the Fig. 6. As shown in the Fig. 6, positive control group had the largest lesions positive staining ($87.6 \pm 5.3\%$) than other treated-groups. And the group-treated with LT-Capsule lowered the lesions positive staining compared with the positive control group ($p < 0.05$). Moreover, in the group-treated with LT-Liposome, the lesion positive staining was further reduced compared with the group-treated with LT-Capsule, but was larger than that in the group-treated with LT-d-rHDL ($p < 0.05$). The Fig. 6 also showed that LT-s-rHDL had smaller lesions positive staining than LT-d-rHDLs ($p < 0.05$). And as the AA modification amount was increased, the lesions positive staining in LT-d-rHDL, 1:20 AA-LT-d-rHDL, 1:10 AA-LT-d-rHDL and 1:5 AA-LT-d-rHDL were gradually decreased, respectively ($p < 0.05$ for LT-d-rHDL compared with 1:10 AA-LT-d-rHDL and $p < 0.05$ for 1:5 AA-LT-d-rHDL compared with 1:10 AA-LT-d-rHDL). Moreover, 1:5 AA-LT-d-rHDL had lower lesions positive staining than LT-s-rHDL ($p < 0.05$), indicating the weakest atherosclerosis.

Mean Intima-Media Thickness

MIT was often examined to evaluate the atherosclerosis extent. The MIT (μm) of aortic tree from each group was visualized by phase contrast light microscopy and calculated. As shown in Fig. 7, MIT of positive control group was markedly increased to 744.1 ± 107.4 μm, compared with 227.5 ± 37.6 μm of negative control group ($p < 0.01$). The MIT of the group-treated with LT-Capsule, LT-Liposome, LT-d-rHDL, 1:20AA-LT-d-rHDL, 1:10AA-LT-d-rHDL, 1:5AA-LT-d-rHDL and LT-s-rHDL were reduced, among them, the MIT of LT-Liposome group was smaller than that of LT-Capsule group ($p < 0.05$), and the MIT of LT-d-rHDL group was further smaller than that of LT-Liposome group ($p < 0.05$), whereas the MIT of LT-d-rHDL group was larger than that of LT-s-rHDL group ($p < 0.05$). Moreover, the MIT of 1:5AA-LT-d-rHDL group was significantly less than that of LT-d-rHDL group ($p < 0.05$).

Immunostaining for MMP-9 and Macrophage

Figure 8 revealed that the MMP-9 protein expression levels varied among different groups. Intensity of green fluorescent signal indicated expression level of MMP-9 protein. As seen from Fig. 8, model group without any intervention exhibited significantly stronger intensive fluorescent signal of MMP-9 protein than normal group ($p < 0.01$). The MMP-9 expression levels indicated by fluorescent signal were decreased in order as follows: LT-Capsule, LT-Liposome, LT-d-rHDL, 1:20AA-LT-d-rHDL, 1:10AA-LT-d-rHDL, LT-s-rHDL and 1:5AA-LT-d-rHDL, respectively.

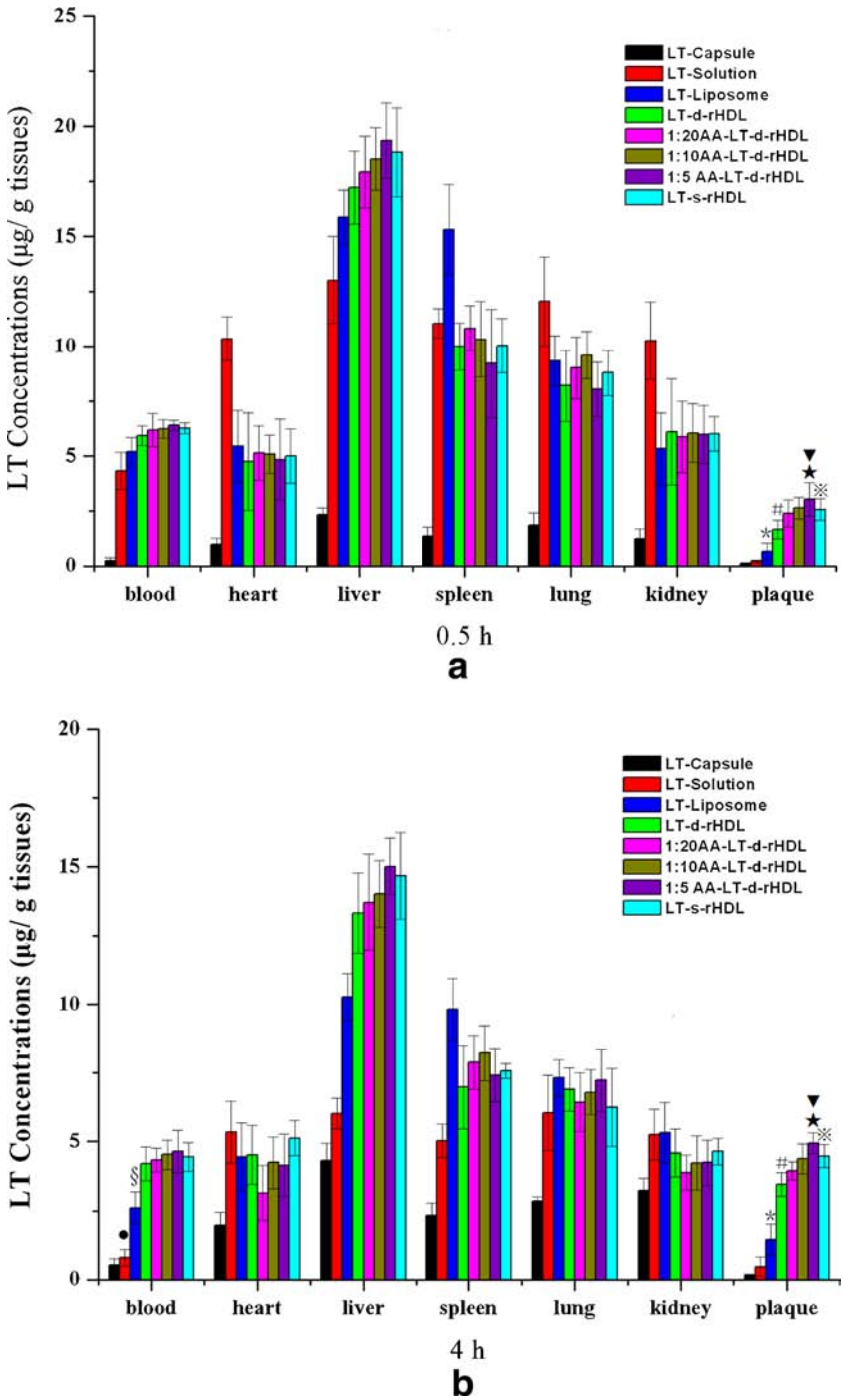

Fig. 5 Biodistribution in atherosclerotic NZW rabbits after administration of LT-Capsule, LT-Solution, LT-Liposome, LT-d-rHDL, 1:20AA-LT-d-rHDL, 1:10AA-LT-d-rHDL, 1:5AA-LT-d-rHDL and LT-s-rHDL, respectively, at 0.5 h (**a**) and 4 h (**b**); (*Black circle*) $p < 0.05$, compared with the LT concentration in plasma of LT-Solution after 4 h with that after 0.5 h, (*Section sign*) $p < 0.05$, compared with LT-Liposome with LT-Solution, *(Asterisk)* $p < 0.05$, compared with LT-Liposome with LT-Solution, (*Number sign*) $p < 0.05$, compared with LT-d-rHDL than LT-Liposome,(*Black star*) $p < 0.05$, compared with 1:5AA-LT-d-rHDL with LT-d-rHDL, (*Black down-pointing triangle*) $p < 0.05$, compared 1:5AA-LT-d-rHDL with LT-s-rHDL, (*Reference mark*) $p < 0.05$, compared LT-s-rHDL with LT-d-rHDL (mean value ± SD, $n = 3$)

The immunohistochemical staining for macrophage from all groups were shown in Fig. 9. Compared with 6.8 ± 2.9% in negative control group, the positive staining area (%) of macrophage was 70.4 ± 6.5% in positive control group ($p < 0.01$). And the positive staining area was slightly decreased to 64.2 ± 7.3% in LT-Capsule group compared with that in positive control group, further decreased in order as follows: LT-Liposome, LT-d-rHDL, 1:20AA-LT-d-rHDL, 1:10AA-LT-d-rHDL, LT-s-rHDL and 1:5AA-LT-d-rHDL, respectively. Among them, the positive staining area of LT-Liposome group was lower than that of LT-Capsule group ($p < 0.05$), the positive staining area of LT-d-rHDL group was further lower than that of LT-Liposome group ($p < 0.05$), whereas the positive staining area of LT-d-rHDL group was higher than that of LT-s-rHDL group ($p < 0.05$). Moreover, the positive staining area of 1:5AA-LT-d-rHDL group was significantly fewer than that of LT-d-rHDL group ($p < 0.05$).

Table III Blood Lipid Levels in Different Experimental Groups (mean value ± SD, $n = 6$)

Groups	TC (mmol/L)	TG (mmol/L)	LDL-C (mmol/L)	HDL-C (mmol/L)
Negative control group	3.47 ± 0.51	0.82 ± 0.47	1.87 ± 0.61	0.71 ± 0.28
Positive control group	43.42 ± 4.98	2.09 ± 1.84	40.24 ± 5.04	0.48 ± 0.15
LT-Capsule	34.98 ± 4.16	1.77 ± 0.53	31.34 ± 3.78	0.49 ± 0.18
LT-Liposome	31.44 ± 3.45	1.72 ± 0.64	30.23 ± 4.22	0.55 ± 0.26
LT-d-rHDL	32.87 ± 3.66	1.54 ± 0.87	29.92 ± 1.56	1.17 ± 0.74
1:20AA-LT-d-rHDL	31.04 ± 2.14	1.55 ± 0.76	28.24 ± 2.42	1.19 ± 0.72
1:10AA-LT-d-rHDL	30.42 ± 2.95	1.42 ± 0.92	27.11 ± 1.88	1.18 ± 0.42
1:5AA-LT-d-rHDL	28.92 ± 2.06	1.47 ± 0.68	26.37 ± 1.15	1.18 ± 0.89
LT-s-rHDL	29.62 ± 2.77	1.50 ± 0.94	27.02 ± 1.60	1.21 ± 0.41

TC total cholesterol, *TG* triglyceride, *LDL-C* low density lipoprotein cholesterol, *HDL-C* high density lipoprotein cholesterol

Western Blotting for MMP-9 and Macrophage

Analogous tendency also appeared in the western bolting analysis of MMP-9 expression and macrophage infiltration (Fig. 10). The level of MMP-9 expression and macrophage in positive control group was obviously higher than those in negative control group, whereas were attenuated to different degrees in those treatment groups. specifically, the MMP-9 expression and macrophage infiltration in the atherosclerotic lesions were further suppressed in order as follows: LT-Capsule, LT-Liposome, LT-d-rHDL, 1:20AA-LT-d-rHDL, 1:10AA-LT-d-rHDL, LT-s-rHDL and 1:5AA-LT-d-rHDL, respectively.

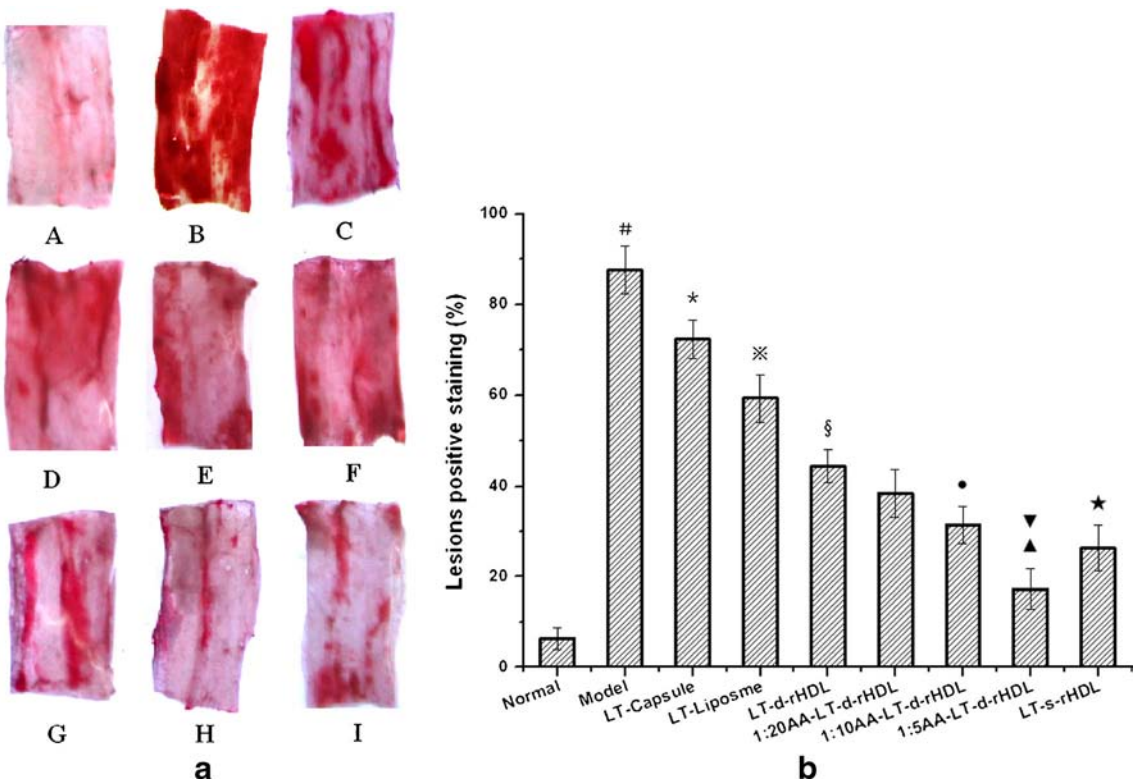

Fig. 6 Oil red O lipid staining of thoracic aorta from different groups depicted in the (**a**), (A) negative control group, (B) positive control group, (C) LT-Capsule, (D) LT-Liposome, (E) LT-d-rHDL, (F) 1:20AA-LT-d-rHDL, (G) 1:10AA-LT-d-rHDL, (H) 1:5AA-LT-d-rHDL and (I) LT-s-rHDL; Quantitative analysis of percentage lesions positive staining in respective groups (**b**); significant differences: (*Number sign*) $p < 0.01$, compared positive control group with negative control group, *(Asterisk)* $p < 0.05$, compared LT-Capsule with positive control group, (*Reference mark*) $p < 0.05$, compared LT-Liposome with LT-Capsule, (*Section sign*) $p < 0.05$, compared LT-d-rHDL with LT-Liposome, (*Black circle*) $p < 0.05$, compared 1:10AA-LT-d-rHDL with LT-d-rHDL, (*Black down-pointing triangle*) $p < 0.05$, compared 1:5AA-LT-d-rHDL with 1:10AA-LT-d-rHDL, (*Black up-pointing triangle*) $p < 0.05$, compared with 1:5AA-LT-d-rHDL with LT-s-rHDL, (*Black star*) $p < 0.05$, compared LT-s-rHDL with LT-d-rHDL (mean value ± SD, $n = 6$)

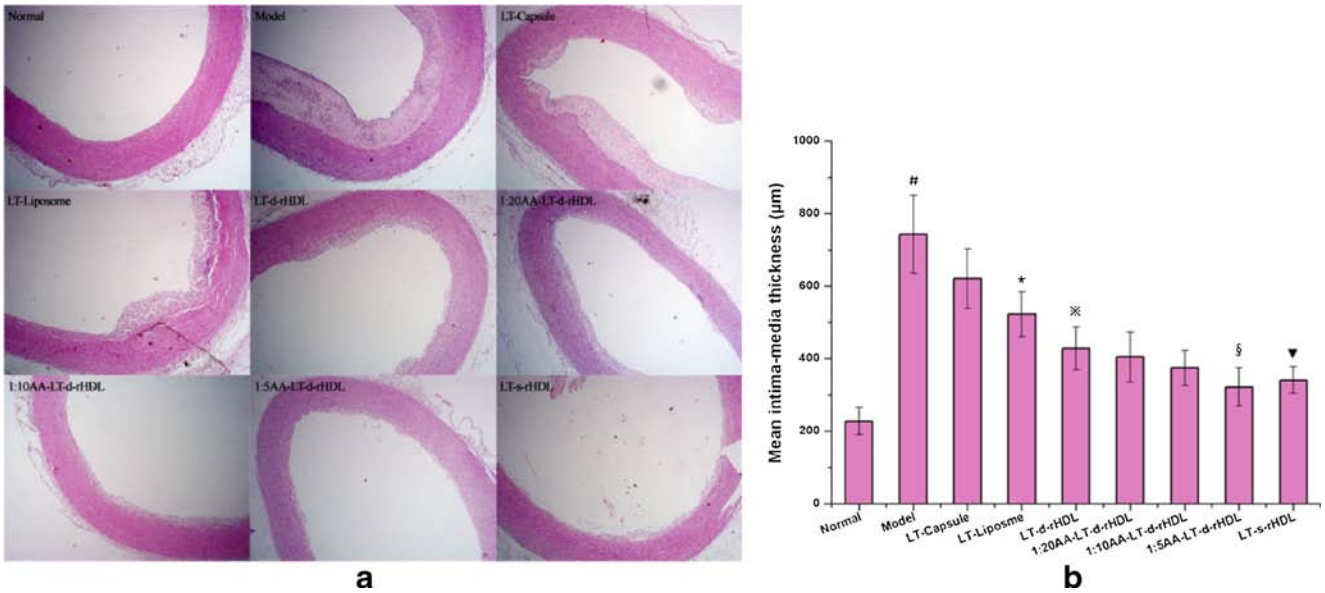

Fig. 7 H&E stained sections of all groups in the (**a**); Mean intima-media thickness (MIT) of different groups (**b**); significant differences: (*Number sign*) $p < 0.01$, compared positive control group with negative control group, (*Asterisk*) $p < 0.05$, compared LT-Liposome with LT-Capsule, (*Reference mark*) $p < 0.05$, compared LT-d-rHDL with LT-Liposome, (*Section sign*) $p < 0.05$, compared 1:5AA-LT-d-rHDL with LT-d-rHDL and (*Black down-pointing triangle*) $p < 0.05$, compared LT-s-rHDL with LT-d-rHDL (mean value ± SD, $n = 6$)

DISCUSSIONS

rHDL could be responsibly considered as an attractive drug delivery system over the other drug carriers consisting of lipids or polymers for prevention and treatment of cardiovascular disease due to its bio-functional properties and excellent attributes such as biodegradability, biocompatibility and receptor-mediated endocytosis, *etc*. However, during our previous researches, undesired drug leakage in the remodeling behaviors of drug-loaded d-rHDL under the action of LCAT and the ensuing reduced efficacy had been observed. The focus of this paper is how to restrain the undesired drug leakage induced by remodeling behaviors and simultaneously retain the exclusive RCT property of d-rHDL. In our earlier report, low reactivity of d-rHDL with LCAT has been obtained through AA insertion into the phospholipids bilayer of d-rHDL (19), which suggested that as the AA insertion amount increased, the reactivity of d-rHDL with LCAT was gradually reduced and the degree of drug leakage was further decreased, thus improving efficacy on inhibiting macrophage-derived foam cell formation. In our current studies, the *in vivo* performances of AA-LT-d-rHDL in atherosclerotic NZW rabbits, such as pharmacokinetic study, atherosclerotic lesions-targeted property and antiatherogenic efficacy, had been elaborately evaluated and compared.

After construction of AA-LT-d-rHDL with different AA amount, including LT-d-rHDL, 1:20AA-LT-d-rHDL, 1:10AA-LT-d-rHDL and 1:5AA-LT-d-rHDL, *in vitro* characterizations had been investigated, which were consistent with our previous report (19). Specifically, the mean sizes were less than 100 nm to avoid the recognition by RES, and the zeta potentials were negative below minus twenty with good stability in suspension. Both EE % and DL % were high to ensure optimal regimen in the following pharmacodynamic experiments.

The results obtained from pharmacokinetic studies in atherosclerotic NZW rabbit suggested that compared with LT-Solution, absolute bioavailability of orally administrated LT-Capsule was merely 4.89%, while $AUC_{0-\infty}$ of other six intravenous LT preparations were improved by 3.44-fold for LT-Liposome, 5.64-fold for LT-d-rHDL, 5.86-fold for 1:20AA-LT-d-rHDL, 6.75-fold for 1:10AA-LT-d-rHDL, 7.35-fold for 1:5AA-LT-d-rHDL and 7.09-fold for LT-s-rHDL respectively, and MRT and CL were correspondingly increased in various degrees, respectively. Among them, compared with LT-Liposome, the MRT of LT-d-rHDL was longer, which was probably due to the extended circulation time of LT-d-rHDL *via* endogenous apoA-I, and the shorter MRT of LT-d-rHDL compared with LT-s-rHDL was probably induced by the drug leakage encountered with LCAT in circulation. Furthermore, as the AA insertion amount increased, $AUC_{0-\infty}$ of AA-LT-d-rHDL was further enlarged than that of LT-d-rHDL, and both MRT and CL were gradually longer, respectively, suggesting that the drug leakage from LT-d-rHDL during the remodeling behaviors aroused by LCAT was inhibited after AA insertion which may lowered the reactivity of LT-d-rHDL with LCAT.

Atherosclerotic lesions targeting properties were examined using *ex vivo* imaging of aortic tree and biodistribution studies, respectively. *Ex vivo* imaging showed that DiR-d-rHDL bound

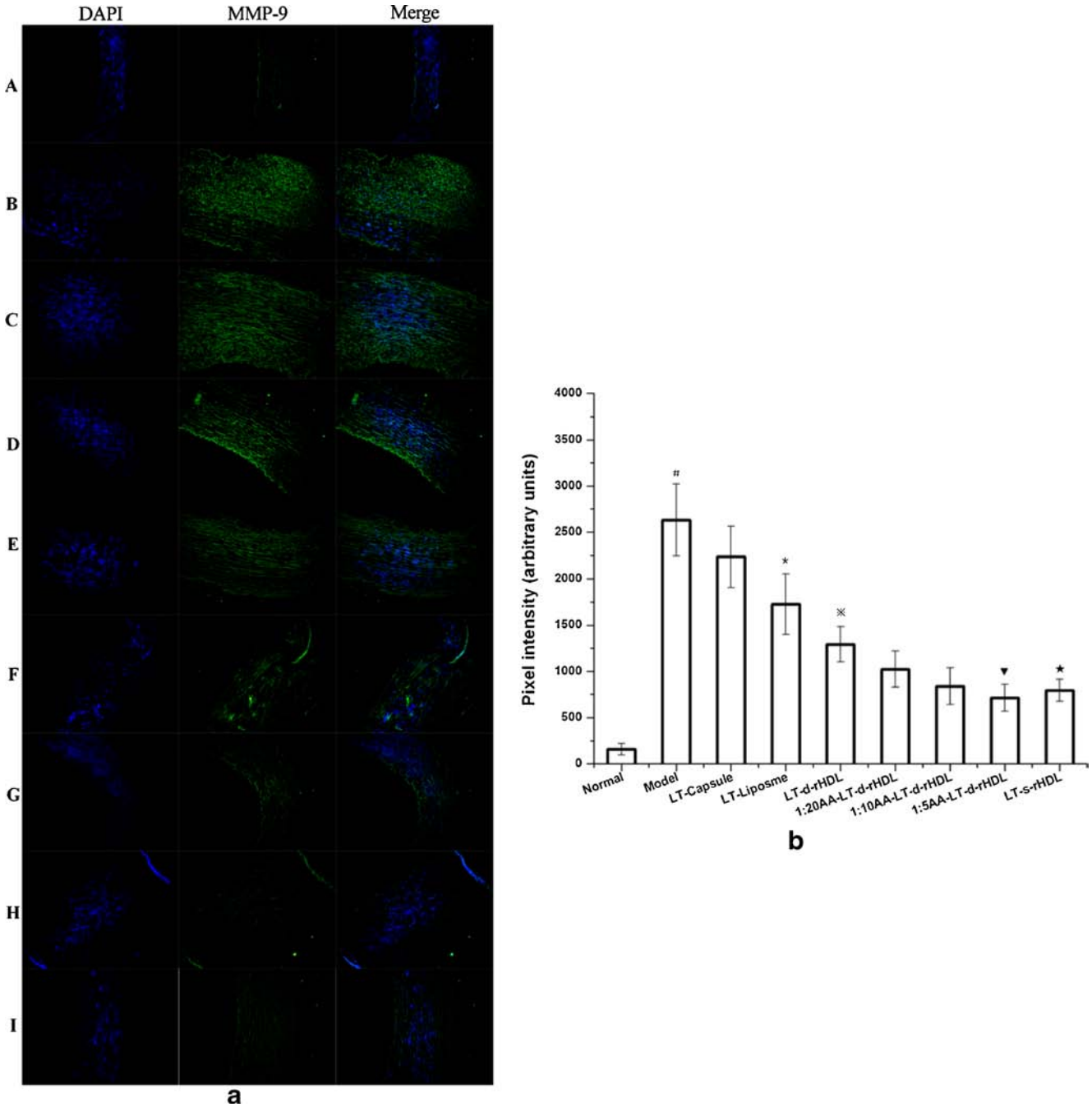

Fig. 8 Immunofluorescence staining indicating the expressions of MMP-9 in aortas from different groups (**a**): (A) negative control group, (B) positive control group, (C) LT-Capsule, (D) LT-Liposome, (E) LT-d-rHDL, (F) 1:20AA-LT-d-rHDL, (G) 1:10AA-LT-d-rHDL, (H) 1:5AA-LT-d-rHDL and (I) LT-s-rHDL; Pixel intensities [arbitrary units] for MMP-9 immunofluorescent intensity of all groups (**b**); significant differences: (*Number sign*) $p < 0.01$, compared positive control group with negative control group, *(Asterisk)* $p < 0.05$, compared LT-Liposome with LT-Capsule, (*Reference mark*) $p < 0.05$, compared LT-d-rHDL with LT-Liposome, (*Black down-pointing triangle*) $p < 0.05$, compared 1:5AA-LT-d-rHDL with LT-d-rHDL and (*Black star*) $p < 0.05$,compared LT-s-rHDL with LT-d-rHDL (mean value ± SD, $n = 6$)

more easily to atherosclerotic lesions than DiR-Liposome did, which was also testified in our previous reports (13), while DiR-s-rHDL had stronger fluorescence intensity than DiR-d-rHDL due to the DiR leakage from DiR-d-rHDL induced by LCAT in circulation. With the increment of AA modification, the fluorescence intensity in atherosclerotic lesions became increasingly stronger in the following order: DiR-d-rHDL, 1:20AA-DiR-d-rHDL, 1:10AA-DiR-d-rHDL and 1:5AA-DiR-d-rHDL, respectively. Coupled with the pharmacokinetics parameters, the enhanced targeting effect after AA modification may result from the reduced DiR leakage from DiR-d-rHDL encountered with LCAT. In addition, 1:5AA-

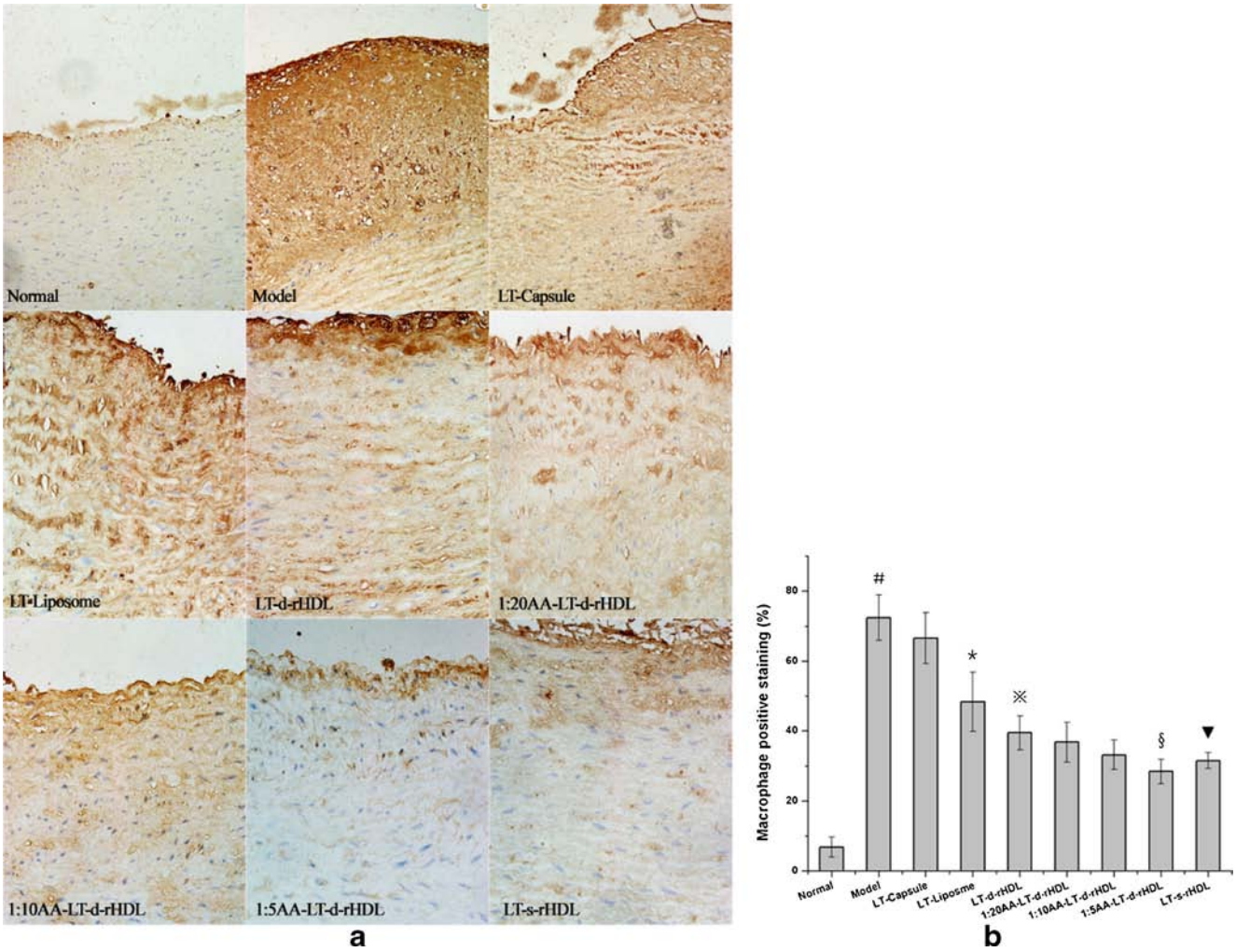

Fig. 9 Immunohistochemical staining of macrophage infiltration in aortas from all groups (**a**); quantitative analysis of macrophage infiltration positive stained area (%) in respective groups (**b**); significant differences: (*Number sign*) $p < 0.01$, compared positive control group with negative control group, *(Asterisk)* $p < 0.05$, compared LT-Liposome with LT-Capsule, (*Reference mark*) $p < 0.05$, compared LT-d-rHDL with LT-Liposome, (*Section sign*) $p < 0.05$, compared 1:5AA-LT-d-rHDL with LT-d-rHDL and (*Black down-pointing triangle*) $p < 0.05$, compared LT-s-rHDL with LT-d-rHDL (mean value ± SD, $n = 6$)

DiR-d-rHDL had significantly stronger fluorescence intensity in the atherosclerotic aortic tree and higher drug distribution in the atherosclerotic lesions than DiR-s-rHDL did, which was probably due to the distinctive phospholipids bilayer in d-rHDL similar to biological membrane but not in the s-rHDL. All the results were also testified in the tissue distribution studies. Briefly, both at 0.5 h and 4 h, the fewest LT accumulation was found in LT-Capsule because of the lowest bioavailability for LT-Capsule. After 4 h administration, the plasma concentration and drug accumulation in all tissues of LT-Solution were significantly lower than other six intravenous LT preparations due to the fastest CL and shortest MRT of LT-Solution. Both LT-Solution and LT-Capsule were widely distributed in most tissues due to freely passive diffusion in circulation. And the LT accumulation in atherosclerotic lesions was larger in LT-Liposome than that in LT-Solution, because LT-Liposome could prolong the half-life, increase AUC of LT and deliver more LT into atherosclerotic lesions, which was ascribed to the enhanced permeation and retention (EPR) effect formed by inflammatory leaky vasculature. As for four kinds of LT-d-rHDLs preparations and LT-s-rHDL, larger LT accumulation in liver and atherosclerotic lesions could be illustrated by SR-BI-mediated uptake, and the tendency of LT accumulation in atherosclerotic lesions among these groups was consistent with that from *ex vivo* imaging of aortic tree. It is notable that the effects of AA modification on atherosclerotic lesions targeting property of LT-d-rHDL could suggest that the AA modification lowered unwanted drug leakage of LT-d-rHDL induced by remodeling behaviors in circulation prior to being delivered to the target, thus leading to efficient drug accumulation in atherosclerotic lesions.

Collectively, there may be several approaches to target atherosclerotic lesions for rHDLs containing LT employed

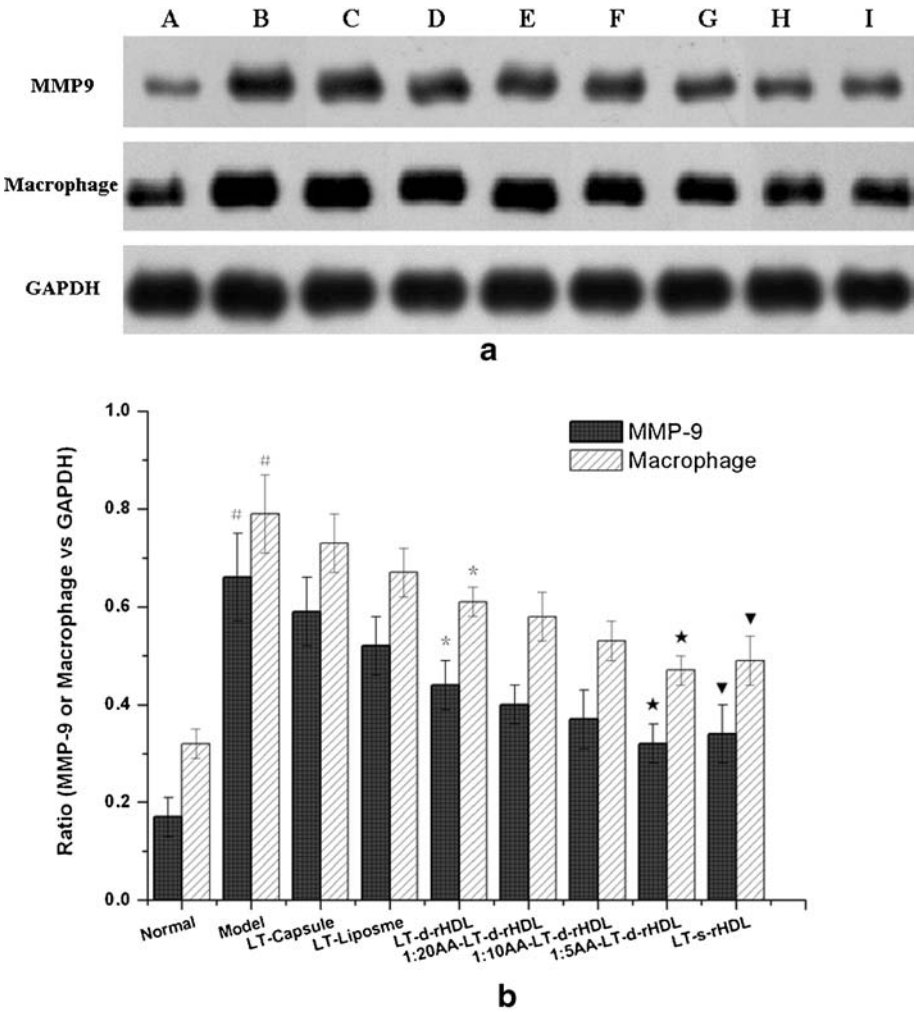

Fig. 10 Western blot analysis for MMP-9 expression and macrophage infiltration in aortic arches from different groups (**a**): (A) negative control group, (B) positive control group, (C) LT-Capsule, (D) LT-Liposome, (E) LT-d-rHDL, (F) 1:20AA-LT-d-rHDL, (G) 1:10AA-LT-d-rHDL, (H) 1:5AA-LT-d-rHDL and (I) LT-s-rHDL; significant differences (**b**): (*Number sign*) $p < 0.05$, compared with model rabbit with normal rabbit, *(Asterisk)* $p < 0.05$, compared with LT-d-rHDL than LT-Liposome, (*Black star*) $p < 0.05$, compared with 1:5AA-LT-d-rHDL with LT-d-rHDL, (*Black down-pointing triangle*) $p < 0.05$, compared LT-s-rHDL with LT-d-rHDL (mean value ± SD, $n = 6$)

in our current studies, which were consistent with our previous researches (13). Firstly, it is well known that atherosclerotic lesions could be a passive target by EPR for the rHDL loaded with LT less than 100 nm in size. Secondly, apoA-I endowed the rHDL containing LT with actively intracellular delivery *via* SR-BI over-expressed in the macrophage abundant in the atherosclerotic lesions, which also had been proposed in other report (25).

As one of the regular medications on atherosclerosis, statins could effectively deplete lipids, alleviate inflammation and attenuate MMPs expression. In the present study, antiatherogenic efficacy of different LT preparations in atherosclerotic NZW rabbit model had been fully characterized by kinds of biochemical indices generally used in evaluating the treatment of atherosclerosis. Specifically, the weakest efficacy of LT-Capsule mainly resulted from the bad bioavailability, while efficacy had been definitely improved in the group-treated with LT-Liposome compared with LT-Capsule, which could be ascribed to larger AUC and longer MRT of LT-Liposome than those of LT-Capsules. Obviously, LT-d-rHDL had significantly stronger efficacy than LT-Liposome because the apoA-I could make the LT-d-rHDL endogenous and deliver more LT into the atherosclerotic lesions *via* efficient receptor-mediated targeting. Moreover, LT-d-rHDL exhibited weaker efficacy than LT-s-rHDL probably because of the drug leakage during remodeling behaviors of LT-d-rHDL encountered with LCAT in circulation, which also could be explained by results from *ex vivo* imaging in the current studies as well as similar tanshinone IIA leakage from d-rHDL induced by LCAT both *in vitro* and *in vivo* studies (13). Furthermore, outcomes from pharmacokinetic studies and atherosclerotic lesions targeting property could explain for more potent antiatherogenic efficacy of 1:5AA-LT-d-rHDL than that of LT-d-rHDL, 1:20AA-LT-d-rHDL and 1:10AA-LT-d-rHDL, respectively.

All the above mentioned observations strongly indicated the AA modification could successfully lower the reactivity of d-rHDL with LCAT and suppress the remodeling reactions, thus preventing the undesired drug leakage, which was also demonstrated in our previous *in vitro* drug release and cellular uptake (19).

Additionally, probably due to the better membrane fusion action (10, 16) and the exclusively atheroprotective RCT effect of d-rHDL (4, 6), 1:5AA-LT-d-rHDL had better antiatherogenic efficacy than LT-s-rHDL. However, probably due to being fed with high fat diet during the intervention, blood lipids such as TC and LDL-C were not lowered down to normal level even in the rabbit-treated with 1:5AA-LT-d-rHDL, which suggested that antiatherogenic efficacies induced by LT preparations employed in our current study were mainly ascribed to not just the lipid-lowering effect of LT, but those antiatherogenic properties of the drug (39, 40), including anti-inflammation, anti-oxidation and improving plaque stability. Collectively, antiatherogenic efficacy studies demonstrated that greatly delivering cardiovascular drug LT into the atherosclerotic lesions using AA-d-rHDL as carriers could efficiently suppress the advancement of atherosclerosis and prevent vulnerable plaques from disruption.

CONCLUSIONS

In summary, AA modification could suppress the remodeling behaviors by lowering the reactivity of LT-d-rHDL with LCAT, reduce undesired drug leakage during circulation, therefore increase the drug accumulation in the target site (atherosclerotic lesions), and exhibit more potent antiatherogenic efficacy in model animal than the conventional LT-d-rHDL. The 1:5AA-LT-d-rHDL had the strongest efficacy among all the AA-LT-d-rHDL with different ratios of AA. However, currently the biggest molar ratio of AA:phospholipids was selected as 1:5 due to the limited AA entrapment capacity in phospholipids bilayer. In order to further increase the drug loading and maintain the discoidal structure of rHDLs, polyunsaturated phospholipids would be considered to modify d-rHDLs in the future.

ACKNOWLEDGMENTS AND DISCLOSURES

This study was financially supported by National Natural Science Foundation of China (No. 81273466), Specialized Research Fund for the Doctoral Program of Higher Education (20120096120005) and A Project Funded by the Priority Academic Program Development of Jiangsu Higher Education Institutions. We also acknowledged kind help in animal study from Institute of Veterinary Medicine (Jiangsu Academy of Agricultural Sciences, Nanjing, Jiangsu) and kind support in evaluation of antiatherogenic efficacies from KeyGEN BioTECH (Changhong Road No. 439, Nanjing, Jiangsu).

REFERENCES

1. Ohtani T, Ueda Y, Mizote I, Oyabu J, Okada K, Hirayama A, *et al.* Number of yellow plaques detected in a coronary artery is associated with future risk of acute coronary syndrome: detection of vulnerable patients by angioscopy. J Am Coll Cardiol. 2006;47(11):2194–200.
2. Mihos CG, Pineda AM, Santana O. Cardiovascular effects of statins, beyond lipid-lowering properties. Pharmacol Res. 2014;88:12–9.
3. Romana B, Batger MA, Prestidge C, Colombo G, Sonvico F. Expanding the therapeutic potential of statins by means of nanotechnology enabled drug delivery systems. Curr Top Med Chem. 2014;14(9):1182–93.
4. Tsompanidi EM, Brinkmeier MS, Fotiadou EH, Giakoumi SM, Kypreos KE. HDL biogenesis and functions: role of HDL quality and quantity in atherosclerosis. Atherosclerosis. 2010;208(1):3–9.
5. Patel S, Drew BG, Nakhla S, Duffy SJ, Murphy AJ, Barter PJ, *et al.* Reconstituted high-density lipoprotein increases plasma high-density lipoprotein anti-inflammatory properties and cholesterol efflux capacity in patients with type 2 diabetes. J Am Coll Cardiol. 2009;53(11):962–71.
6. Nicholls SJ, Dusting GJ, Cutri B, Bao S, Drummond GR, Rye K-A, *et al.* Reconstituted high-density lipoproteins inhibit the acute pro-oxidant and proinflammatory vascular changes induced by a periarterial collar in normocholesterolemic rabbits. Circulation. 2005;111(12):1543–50.
7. Mooberry LK, Nair M, Paranjape S, McConathy WJ, Lacko AG. Receptor mediated uptake of paclitaxel from a synthetic high density lipoprotein nanocarrier. J Drug Target. 2010;18(1):53–8.
8. Ding Y, Wang W, Feng M, Wang Y, Zhou J, Ding X, *et al.* A biomimetic nanovector-mediated targeted cholesterol-conjugated siRNA delivery for tumor gene therapy. Biomaterials. 2012;33(34):8893–905.
9. McMahon KM, Thaxton CS. High-density lipoproteins for the systemic delivery of short interfering RNA. Expert Opin Drug Del. 2014;11(2):231–47.
10. Zhang W, Xiao Y, Liu J, Wu Z, Gu X, Xu Y, *et al.* Structure and remodeling behavior of drug-loaded high density lipoproteins and their atherosclerotic plaque targeting mechanism in foam cell model. Int J Pharm. 2011;419(1):314–21.
11. Liu L, He H, Zhang M, Zhang S, Zhang W, Liu J. Hyaluronic acid-decorated reconstituted high density lipoprotein targeting atherosclerotic lesions. Biomaterials. 2014;35(27):8002–14.
12. Damiano MG, Mutharasan RK, Tripathy S, McMahon KM, Thaxton CS. Templated high density lipoprotein nanoparticles as potential therapies and for molecular delivery. Adv Drug Deliver Rev. 2013;65(5):649–62.
13. Zhang W, He H, Liu J, Wang J, Zhang S, Zhang S, *et al.* Pharmacokinetics and atherosclerotic lesions targeting effects of tanshinone IIA discoidal and spherical biomimetic high density lipoproteins. Biomaterials. 2013;34(1):306–19.
14. Zhang W, Li J, Liu J, Wu Z, Xu Y, Wang J. Tanshinone IIA-loaded reconstituted high density lipoproteins: atherosclerotic plaque targeting mechanism in a foam cell model and pharmacokinetics in rabbits. Pharmazie. 2012;67(4):324–30.
15. Zhang W, Gu X, Bai H, Yang R, Dong C, Liu J. Nanostructured lipid carriers constituted from high-density lipoprotein components for delivery of a lipophilic cardiovascular drug. Int J Pharm. 2010;391(1):313–21.
16. Jia J, Xiao Y, Liu J, Zhang W, He H, Chen L, *et al.* Preparation, characterizations, and in vitro metabolic processes of paclitaxel-loaded discoidal recombinant high-density lipoproteins. J Pharm Sci. 2012;101(8):2900–8.

17. Wang J, Jia J, Liu J, He H, Zhang W, Li Z. Tumor targeting effects of a novel modified paclitaxel-loaded discoidal mimic high density lipoproteins. Drug Deliv. 2013;20(8):356–63.
18. Zhang M, Jia J, Liu J, He H, Liu L. A novel modified paclitaxel-loaded discoidal recombinant high-density lipoproteins: preparation, characterizations and in vivo evaluation. AJPS. 2013;8(1): 11–8.
19. He H, Liu L, Bai H, Wang J, Zhang Y, Zhang W, *et al.* Arachidonic acid-modified lovastatin discoidal reconstituted high density lipoprotein markedly decreases the drug leakage during the remodeling behaviors induced by lecithin cholesterol acyltransferase. Pharm Res. 2014;31(7):1689–709.
20. Sparks DL, Chatterjee C, Young E, Renwick J, Pandey NR. Lipoprotein charge and vascular lipid metabolism. Chem Phys Lipids. 2008;154(1):1–6.
21. Huggins KW, Curtiss LK, Gebre AK, Parks JS. Effect of long chain polyunsaturated fatty acids in the sn-2 position of phosphatidylcholine on the interaction with recombinant high density lipoprotein apolipoprotein AI. J Lipid Res. 1998;39(12):2423–31.
22. Parks JS, Huggins KW, Gebre AK, Burleson ER. Phosphatidylcholine fluidity and structure affect lecithin: cholesterol acyltransferase activity. J Lipid Res. 2000;41(4):546–53.
23. Chen C-C, Tsai T-H, Huang Z-R, Fang J-Y. Effects of lipophilic emulsifiers on the oral administration of lovastatin from nanostructured lipid carriers: physicochemical characterization and pharmacokinetics. Eur J Pharm Biopharm. 2010;74(3):474–82.
24. VanderLaan PA, Reardon CA, Getz GS. Site specificity of atherosclerosis site-selective responses to atherosclerotic modulators. Arterioscl Throm Vas. 2004;24(1):12–22.
25. Frias JC, Williams KJ, Fisher EA, Fayad ZA. Recombinant HDL-like nanoparticles: a specific contrast agent for MRI of atherosclerotic plaques. J Am Chem Soc. 2004;126(50):16316–7.
26. Zhang C, Qu G, Sun Y, Wu X, Yao Z, Guo Q, *et al.* Pharmacokinetics, biodistribution, efficacy and safety of N-octyl-O-sulfate chitosan micelles loaded with paclitaxel. Biomaterials. 2008;29(9):1233–41.
27. Shi Z-S, Loh Y, Duckwiler GR, Jahan R, Viñuela F. Balloon-assisted transarterial embolization of intracranial dural arteriovenous fistulas: Clinical article. J Neurosurg. 2009;110(5):921–8.
28. Hernández-Presa MA, Bustos C, Ortego M, Tuñón J, Ortega L, Egido J. ACE inhibitor quinapril reduces the arterial expression of NF-κB-dependent proinflammatory factors but not of collagen I in a rabbit model of atherosclerosis. Am J Pathol. 1998;153(6):1825–37.
29. Pols TW, Bonta PI, Pires NM, Otermin I, Vos M, de Vries MR, *et al.* 6-mercaptopurine inhibits atherosclerosis in apolipoprotein e* 3-leiden transgenic mice through atheroprotective actions on monocytes and macrophages. Arterioscl Throm Vas. 2010;30(8): 1591–7.
30. Chen WQ, Zhang L, Liu YF, Chen L, Ji XP, Zhang M, *et al.* Prediction of atherosclerotic plaque ruptures with high-frequency ultrasound imaging and serum inflammatory markers. Am J Physiol-Heart C. 2007;293(5):H2836–H44.
31. Daley S, Herderick E, Cornhill J, Rogers K. Cholesterol-fed and casein-fed rabbit models of atherosclerosis. Part 1: Differing lesion area and volume despite equal plasma cholesterol levels. Arterioscl Throm Vas. 1994;14(1):95–104.
32. Anderson JL, Muhlestein JB, Carlquist J, Allen A, Trehan S, Nielson C, *et al.* Randomized secondary prevention trial of azithromycin in patients with coronary artery disease and Serological evidence for chlamydia pneumoniae infection the azithromycin in coronary artery disease: elimination of myocardial infection with chlamydia (ACADEMIC) study. Circulation. 1999;99(12):1540–7.
33. Dong B, Zhang C, Feng JB, Zhao YX, Li SY, Yang YP, *et al.* Overexpression of ACE2 enhances plaque stability in a rabbit model of atherosclerosis. Arterioscl Throm Vas. 2008;28(7):1270–6.
34. Cipollone F, Prontera C, Pini B, Marini M, Fazia M, De Cesare D, *et al.* Overexpression of functionally coupled cyclooxygenase-2 and prostaglandin E synthase in symptomatic atherosclerotic plaques as a basis of prostaglandin E2-dependent plaque instability. Circulation. 2001;104(8):921–7.
35. Li D, Patel AR, Klibanov AL, Kramer CM, Ruiz M, Kang B-Y, *et al.* Molecular imaging of atherosclerotic plaques targeted to oxidized LDL receptor LOX-1 by SPECT/CT and magnetic resonance. Circ-Cardiovasc Imag. 2010;3(4):464–72.
36. Greenstein SM, Sun S, Calderon TM, Kim DY, Schreiber TC, Schechner RS, *et al.* Mycophenolate mofetil treatment reduces atherosclerosis in the cholesterol-fed rabbit. J Surg Res. 2000;91(2): 123–9.
37. Hernández-Presa MA, Ortego M, Tuñón J, Martín-Ventura JL, Mas S, Blanco-Colio LM, *et al.* Simvastatin reduces NF-κB activity in peripheral mononuclear and in plaque cells of rabbit atheroma more markedly than lipid lowering diet. Cardiovasc Res. 2003;57(1):168–77.
38. Yu K-N, Minai-Tehrani A, Chang S-H, Hwang S-K, Hong S-H, Kim J-E, *et al.* Aerosol delivery of small hairpin osteopontin blocks pulmonary metastasis of breast cancer in mice. PLoS One. 2010;5(12):e15623.
39. Hrboticky N, Draude G, Hapfelmeier G, Lorenz R, Weber P. Lovastatin decreases the receptor-mediated degradation of acetylated and oxidized LDLs in human blood monocytes during the early stage of differentiation into macrophages. Arterioscl Throm Vas. 1999;19(5):1267–75.
40. Lin R, Liu J, Peng N, Yang G, Gan W, Wang W. Lovastatin reduces nuclear factor KAPPA. B activation induced by C-reactive protein in human vascular endothelial cells. Biol Pharm Bull. 2005;28(9):1630–4.